Terahertz Excitonic Response of Isolated Single-Walled Carbon Nanotubes

Xinlong Xu, Ken Chuang, Robin J. Nicholas, Michael B. Johnston, and Laura M. Herz*

Clarendon Laboratory, Department of Physics, Oxford University, Parks Road, Oxford OX1 3PU, United Kingdom

Received: July 28, 2009

We have investigated the ultrafast far-infrared transmission of isolated single-walled carbon nanotubes using optical-pump THz-probe spectroscopy. The THz dielectric response is dominated by excitons with an initial, rapid decay due to Auger recombination followed by a slow decay of isolated single excitons. Frequency-dependent analysis of the photoinduced dielectric function suggest an internal excitonic excitation at ∼11 meV with further low-frequency (∼0.6 and 1.4 THz) absorption features at high densities ascribed to exciton complexes. A featureless conductivity bleaching is attributed to an exciton-induced reduction in the mobility of free carriers caused by phase-space filling.

Introduction

Single-walled carbon nanotubes (SWNTs) have received considerable interest because of their potential for implementation in nanoelectronic and photovoltaic devices.[1,2] As fundamentally one-dimensional systems, SWNTs also offer great opportunities for exploration of nanoscale effects. Although photoexcited species play an important role in the electronic and optical properties of SWNTs, the nature of the excitations generated is still a matter of intense debate. Some recent studies have concluded that bound electron−hole pairs (excitons) are the primary excitations in SWNTs,[3−5] with the observation of low photoluminescence (PL) quantum efficiencies[6] pointing toward the presence of highly efficient nonradiative processes. Other studies[7,8] have indicated that charged carriers (electrons or holes) might be the initially excited species. Coulomb interactions are known to be particularly strong in SWNTs because of their one-dimensional nature, and it has also been suggested that phonons are involved in the electronic dynamics.[5,9,10] Transient optical-pump terahertz (THz)-probe (OPTP) spectroscopy provides an ideal tool to resolve such issues as it permits the simultaneous probing of both real and imaginary parts of the dielectric function with good time resolution and across a broad frequency band.[11] Two independent investigations based on OPTP measurement on SWNT films have recently come to opposite conclusions. While one study found an absence of free-carrier response and proposed that photogenerated changes in THz transmission are caused by bleaching of optical transitions in small-gap tubes,[12] another group reported highly efficient generation of free charges from exciton dissociation and subsequent interaction with the THz probe.[13] Both groups, however, studied nanotube films for which significant intertube interactions were expected to occur.

In this paper, we present an ultrafast OPTP study of SWNTs that are fully isolated in a gelatin matrix. We show that in the absence of intertube interactions the intrinsic properties of SWNTs can be measured by selective excitation of semiconducting SWNTs, which leads to transient changes in the THz transmission caused by excitonic transitions. Our measurements indicate that as the number of excitations on a single nanotube exceeds one, exciton−exciton interactions lead to a short-lived, fluence-dependent component of the transient THz dielectric response. At later times (>10 ps), a slow decay of the THz transmission signal is observed, which is in agreement with the known high stability of excitons in isolated SWNTs. We are able to describe the measured frequency-dependence of the transient changes in dielectric function by a combination of an intraexcitonic Lorentzian resonance and a featureless background arising from bleaching effects. In addition to this response, two lower energy absorptions are observed in the multiexciton regime that are ascribed to the presence of exciton complexes.

Experimental Section

The SWNTs under investigation were grown by Carbon Nanotechnologies Inc., using the high-pressure-carbon-monoxide (HiPCO) technique. Strong sonication with the surfactant sodium dodecylbenzene sulfate and ultracentrifugation[14] in solution were used to produce isolated SWNTs, after which gelatin was added as a matrix to prevent aggregation. The SWNT-gelatin solution was deposited on a substrate, desiccated in air and then lifted off to provide free-standing SWNTs-gelatin films. PL excitation maps of the films (Figure 1(a)) show strong, well-defined optical transitions between van Hove singularities concomitant with an absence of intertube excitation transfer and the presence of isolated SWNTs.[14] The OPTP setup used has been described in detail elsewhere.[15] The experiment was based on a Ti:sapphire regenerative amplifier with a central wavelength of 800 nm, a repetition rate of 1 kHz, and a pulse width of 40 fs. The amplifier output was divided into three beams, one for THz wave generation based on optical rectification in ZnTe, the second for THz wave detection using the linear electro-optical effect in ZnTe, and the third for excitation of the samples. All optical elements related to the generation and detection of THz radiation were enclosed in a vacuum chamber to limit absorption by water. It has been shown recently that the intersubband relaxation in SWNTs occurs on an ultrafast (∼40 fs) time scale.[5] Thus our measurement scheme ensures that the ground-state dynamics are probed despite the initial optical pumping into higher-lying states.

Results and Discussion

Figure 1 presents the differential transmission $\delta T(t)/T$ of THz radiation as a function of time after pumping with 800 nm

* To whom correspondence should be addressed: E-mail: l.herz@physics.ox.ac.uk.

10.1021/jp907195t CCC: $40.75
Published on Web 09/17/2009

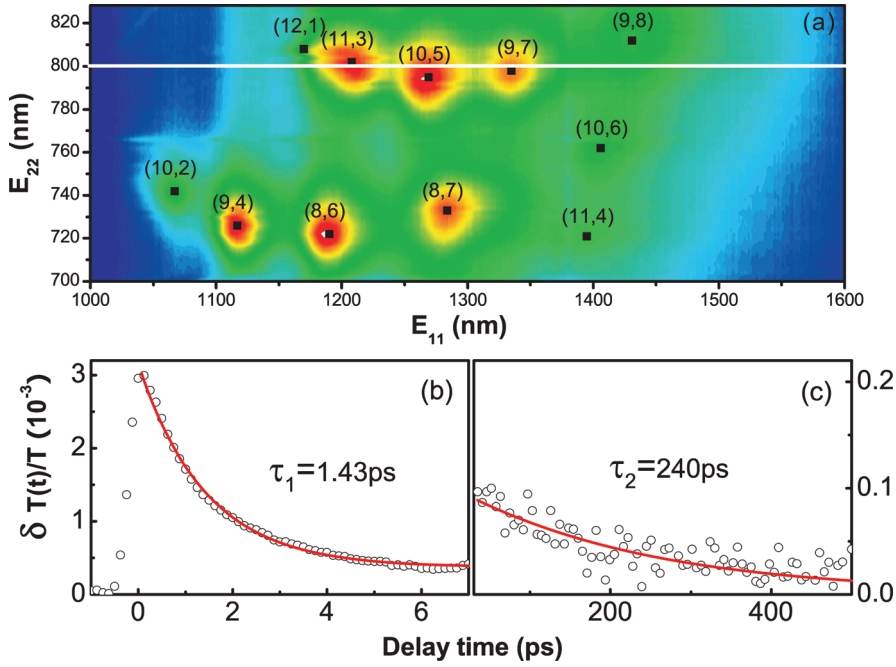

Figure 1. (a) PL excitation map of the SWNT-gelatin film showing the PL intensity emitted from the E_{11} transition after excitation of the E_{22} transition. (Bottom) Optically induced differential THz transmission as a function of time after excitation with a photon fluence of 22 μJ cm^{-2} showing (b) an initial rapid decay (circles) fitted with a single exponential decay (solid line) and (c) the slow subsequent single exponential decay.

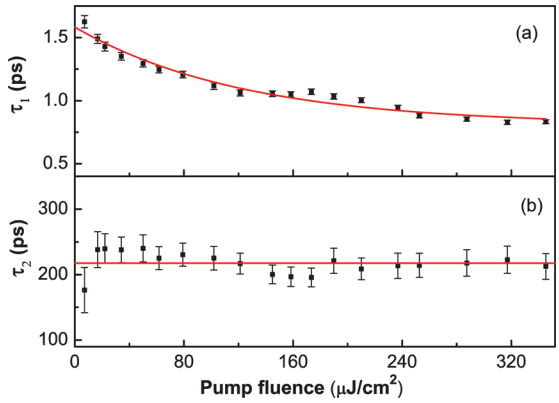

Figure 2. Pump-fluence dependence of the decay time constants extracted from monoexponential fits to the THz transmission transients over (a) the initial (0−6 ps) decay and (b) the subsequent slow (30−500 ps) decay component. The solid lines are guides to the eye.

radiation, which excites primarily the branch of nanotubes corresponding to the chiral indices (9,7), (10,5), and (11,3)[14] as can be seen from the PL excitation map (Figure 1a). No metallic nanotubes will be excited as 800 nm radiation is resonant only with metallic nanotubes with diameters in the range 1.5−1.6 nm, which are not present in significant quantitities in HiPCO material.[16] Since no signal was observed upon optical excitation of pure gelatin films, the displayed transients must arise from the photoinduced THz response of the incorporated SWNTs. The photoinduced change in THz transmission decays on two distinct time scales, a fast initial component (Figure 1b) with a picosecond time scale and a slower decay (Figure 1c) lasting a few hundred picoseconds. Monoexponential fits to the fast and the slow decay components allowed the respective decay times τ_1 and τ_2 to be extracted, which are shown in Figure 2 as a function of excitation fluence. The lifetime of the fast initial decay is dependent on the pump intensity, decreasing from ~1.7 ps at an excitation fluence of 10 μJ cm^{-2} to ~0.8 ps at a fluence of 350 μJ cm^{-2}. The longer-lived component of the differential transmission, on the other hand, has a fluence-independent decay constant of ~220 ps over the same range of fluences.

For well-isolated SWNTs at low excitation intensities, time-resolved PL studies have always shown excitonic lifetimes of order ~100 ps.[3−5,17] The similarity of this lifetime to the slow decay component we observe, and its independence of the initial pump fluence (Figure 2b), strongly suggests that single excitons are the predominant contributors to the THz transmission changes at times larger than a few picoseconds after excitation. Fast initial decay components in the excitation dynamics (Figure 2a) are typically observed when either bundling of SWNTs leads to formation of heterojuctions between different types of SWNTs[8,12] or at high excitation intensities where multiple excitons are created on individual nanotubes leading to Auger recombination.[3,6,18] In the present case, the tubes are well isolated and a dominant excitonic contribution is expected. We estimate that on average one exciton is generated per nanotube for an excitation pulse of 11 μJ cm^{-2}. For most of the excitation fluences studied here, multiple excitons are thus initially present on each tube, leading to exciton−exciton annihilation dynamics that become increasingly fast as the density of initially generated excitons is increased. While PL measurements have shown that excitons are the primary photogenerated species in SWNT, they do not provide direct information on whether free charges are also generated as has been previously suggested.[12,13] THz transmission studies, on the other hand, are highly sensitive probes of both photoinduced conductivity changes[15] and excitonic polarizibilities[11] and therefore allow an assessment of the contributions from both of the photogenerated species.

Figure 3 displays the THz-frequency dependence of the changes in complex dielectric function $\Delta\varepsilon$ at 1.4 and 20 ps after excitation, extracted from the measured differential transmission spectra using the analysis presented by Knoesel et al.[19] The spectra display a significant negative imaginary part that does not follow a simple Drude behavior. At the early times, the dielectric function also shows some additional sharper features at around 0.6 and 1.4 THz, which gradually disappear over the

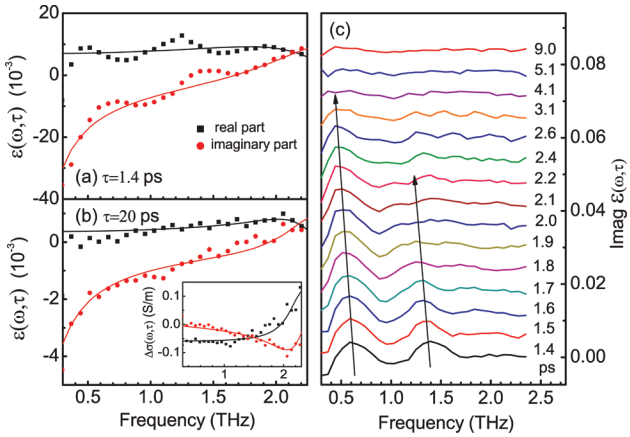

Figure 3. THz complex dielectric function of SWNTs measured at (a) 1.4 and (b) 20 ps after excitation at a fluence of 158 μJ cm^{-2}. The insert in (b) shows the matching photoinduced conductivity $\Delta\sigma = -i\omega\varepsilon_0\varepsilon$. The solid lines represent fits of eq 1 to the data. Panel (c) shows the oscillatory component to the data for various time delays in units of picoseconds after excitation, extracted by subtraction of the fitted lines from the imaginary part of the data. Values are offset by 0.006 between successive curves for clarity of viewing. The arrows indicate the temporal shift in the position of the maxima.

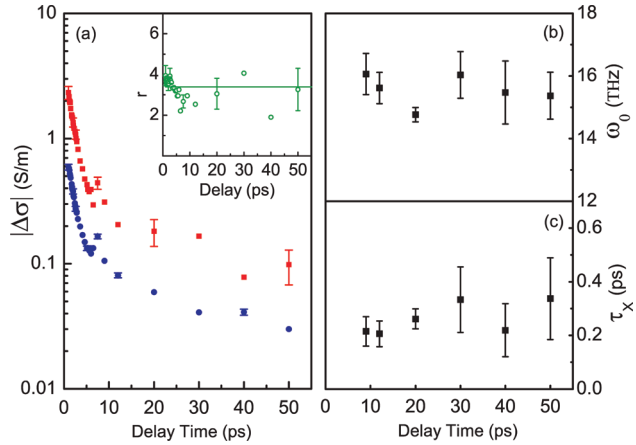

Figure 4. Parameters extracted from fits of eq 1 to the complex dielectric function as shown in Figure 3. (a) Excitonic resonance amplitude, $\varepsilon_0\tau_x f$ (squares) and charge carrier conductivity change, $|\Delta\sigma_c|$ (circles). The inset shows the ratio r between the two quantities. (b) Excitonic resonance frequency ω_0 and (c) excitonic damping time, shown as a function of time after excitation.

first few picoseconds after excitation. These will be discussed separately after we have addressed the underlying response.

For a more quantitative analysis of the mechanisms leading to changes in THz transmission, we have modeled the data using a Lorentzian resonance formula in analogy to the approach taken in previous studies.[12,13] We find that for the well-isolated SWNT films investigated, the best fit to the data is provided by the sum of a resonance term and a bleaching response associated with changes in charge conductivity

$$\Delta\varepsilon(\tau,\omega) = \frac{f}{\omega_0^2 - \omega^2 - i\omega/\tau_x} + i\frac{\Delta\sigma_c}{\varepsilon_0\omega} \qquad (1)$$

Here, ω_0 is the resonance frequency, f is the oscillator strength, τ_x is the damping constant associated with the Lorentzian resonance, and $\Delta\sigma_c$ is a spectrally uniform photoinduced change in the conductivity of the tubes. Fits based on this model (solid lines in Figure 3a,b) are in good agreement with the experimental data with the extracted fitting parameters displayed in Figure 4 as a function of time after excitation.

The amplitudes $|\Delta\sigma_c|$ and $\varepsilon_0\tau_x f$ of the two mechanisms both show an initial fast drop, which slows significantly once the initial signal (corresponding to an average density of 14 excitons per tube) has decayed by about 1 order of magnitude. For both components, the ensuing longer-lived decay again carries the lifetime signature of isolated excitons on SWNTs.[3−5,17] Figure 4a shows that for the entire measurable range of a few hundred picoseconds after excitation, the ratio $\varepsilon_0\tau_x f/|\Delta\sigma_c| \sim 3.4$, suggesting that both terms are the result of the same mechanism, that is, the photogeneration of an exciton population. These findings differ from earlier observations by Perfetti et al. who investigated the THz transmission dynamics of partly bundled SWNTs and found contributions from two different mechanisms, which they concluded to be bleaching of optical transitions in small-gap SWNTs and absorption by localized carriers.[12] Here we show that for fully isolated tubes and selective excitation of semiconducting tubes, only the excitons contribute to the THz absorption.

The extracted frequency of the Lorentzian resonance, ω_0, (Figure 4b) is 15 THz (ν = 2.4 THz, Energy = 11 meV) independent of delay time. This resonance therefore most likely corresponds to an internal excitonic transition, probably within the exciton singlet manifold, where energy separations lie within the THz spectral region.[20−24] Given the high stability[25] of excitons in SWNTs, such internal transitions between bright and dark excitonic levels are very likely.[18,21,22] At present, the full internal spectrum of the excitions remains uncertain with most reported values for the singlet bright-dark exciton splitting on the order of 5−10 meV[21−24,26,27] and other splittings within the singlet manifold calculated to be up to 30 meV.[21,22] The extracted excitonic scattering time τ_x is found to be of the order of 200 fs (Figure 4c), which may for example arise from coupling to defects or intraexcitonic transitions. This value is comparable to the broadening found for direct excitonic transitions observed[24] in insolated single nanotubes.

The second, featureless contribution to the spectra, given by $\Delta\sigma_c$, is peculiar as it displays the same dynamics as the excitonic resonance feature but is negative and describes a charge conductivity response. Within the approximations of the Drude model such featureless backgrounds arise when $\omega\tau < 1$, which Hilt et al. have attributed to the localization of charge carriers.[28] We propose that this feature is caused by an exciton-induced reduction in the intrinsic conductivity of the sample. Unintentional doping (e.g., through reaction with ambient oxygen) generally leads to the presence of charges even in semiconducting SWNTs.[29] While excitons are neutral species, the generation of electron−hole pairs causes a local filling of phase space available near the band edge, which will in turn promote existing free charges to states associated with lower mobility and can act as a local barrier to charge transport. Consequently, a photoinduced reduction in conductivity is observed that displays the same dynamic trends as the resonance signal of the photogenerated excitons.

We note that the spectral shapes of the dielectric function we observe fundamentally differ from those measured previously by Beard et al. for SWNT films that contained electrical pathways for conduction.[13] These authors reported a THz signature of free charges and concluded that charge-carriers were photogenerated with over 60% yields in SWNT films. Efficient exciton dissociation into free charges is expected to occur at the heterojunctions formed between nanotubes of different types;

however, as we demonstrate here, such exciton dissociation is absent when the tubes are carefully isolated.

To examine the additional oscillatory behavior that is superimposed on the dielectric function, we subtracted from the data the fits based on eq 1 as described above. Figure 3c shows the resulting residual component of the imaginary part of the dielectric function for a range of times after excitation. Two absorption maxima can be clearly observed at about 0.6 and 1.4 THz, (2.5 and 5.7 meV) whose amplitude decay matches the fast initial decay of the differential THz transmission shown in Figure 1b and whose peak position shifts slightly toward lower energy with time. These peaks are not the result of artifacts arising from pump−probe overlap on the sample as for our experiments the THz pulse has a duration of 1 ps and the pump a duration of 40 fs. The correspondence with the fast decay component of the signal implies that these features require the presence of multiple excitons within the nanotubes and that the excitation energies are exciton-density dependent. This suggests that the origin of these transitions may be related to the formation of exciton complexes such as biexcitons for which there is currently little that has been predicted or is known.

Summary

In conclusion, the transient THz measurements and analysis presented here allow the contributions of both excitons and free carriers to be detected but demonstrate unambiguously that the optical response of isolated, large-gap semiconducting carbon nanotubes can be described entirely in terms of the properties of excitons as the only photogenerated species. An initial fast decay induced by many-exciton decay processes is followed by a slower decay on a time scale of hundreds of picoseconds compatible with the presence of stable, isolated excitons at low photoexcitation densities. Internal exciton excitations with a resonance energy of ∼11 meV are identified, which are independent of the exciton density. In addition, a negative (bleaching) contribution to the dielectric function is found to correlate closely with the excitonic response and is attributed to phase-space filling affecting the conductivity of nonoptically induced free charge carriers. In the high excitation density regime, further low-energy excitations are observed that we tentatively attribute to exciton complex excitations.

Acknowledgment. The authors thank the EPSRC for funding.

References and Notes

(1) Saito, R.; Dresselhaus, G.; Dresselhaus, M. S. *Physical Properties of Carbon Nanotubes*; Imperial College Press: London, 1999.

(2) Kymakis, E.; Alexandrou, I.; Amaratunga, G. A. J. *J. Appl. Phys.* **2003**, *93*, 1764.

(3) Huang, L. B.; Krauss, T. D. *Phys. Rev. Lett.* **2006**, *96*, 057407.

(4) Korovyanko, O. J.; Sheng, C. X.; Vardeny, Z. V.; Dalton, A. B.; Baughman, R. H. *Phys. Rev. Lett.* **2004**, *92*, 017403.

(5) Manzoni, C.; Gambetta, A.; Menna, E.; Meneghetti, M.; Lanzani, G.; Cerullo, G. *Phys. Rev. Lett.* **2005**, *94*, 207401.

(6) Wang, F.; Dukovic, G.; Brus, L. E.; Heinz, T. F. *Phys. Rev. Lett.* **2004**, *92*, 177401.

(7) Ostojic, G. N.; Zaric, S.; Kono, J.; Strano, M. S.; Moore, V. C.; Hauge, R. H.; Smalley, R. E. *Phys. Rev. Lett.* **2004**, *92*, 117402.

(8) Lauret, J. S.; Voisin, C.; Cassabois, G.; Delalande, C.; Roussignol, P.; Jost, O.; Capes, L. *Phys. Rev. Lett.* **2003**, *90*, 057404.

(9) Lim, Y. S.; Yee, K. J.; Kim, J. H.; Haroz, E. H.; Shaver, J.; Kono, J.; Doorn, S. K.; Hauge, R. H.; Smalley, R. E. *Nano Lett.* **2006**, *6*, 2696.

(10) Chou, S. G.; Plentz, F.; Jiang, J.; Saito, R.; Nezich, D.; Ribeiro, H. B.; Jorio, A.; Pimenta, M. A.; Samsonidze, G. G.; Santos, A. P.; Zheng, M.; Onoa, G. B.; Semke, E. D.; Dresselhaus, G.; Dresselhaus, M. S. *Phys. Rev. Lett.* **2005**, *94*, 127402.

(11) Hendry, E.; Schins, J. M.; Candeias, L. P.; Siebbeles, L. D. A.; Bonn, M. *Phys. Rev. Lett.* **2004**, *92*, 196601.

(12) Perfetti, L.; Kampfrath, T.; Schapper, F.; Hagen, A.; Hertel, T.; Aguirre, C. M.; Desjardins, P.; Martel, R.; Frischkorn, C.; Wolf, M. *Phys. Rev. Lett.* **2006**, *96*, 027401.

(13) Beard, M. C.; Blackburn, J. L.; Heben, M. J. *Nano Lett.* **2008**, *8*, 4238.

(14) Bachilo, S. M.; Strano, M. S.; Kittrell, C.; Hauge, R. H.; Smalley, R. E.; Weisman, R. B. *Science* **2002**, *298*, 2361.

(15) Parkinson, P.; Lloyd-Hughes, J.; Johnston, M. B.; Herz, L. M. *Phys. Rev. B* **2008**, *78*, 115321.

(16) Fantini, C.; Jorio, A.; Souza, M.; Strano, M. S.; Dresselhaus, M. S.; Pimenta, M. A. *Phys. Rev. Lett.* **2004**, *93*, 147406.

(17) Hagen, A.; Steiner, M.; Raschke, M. B.; Lienau, C.; Hertel, T.; Qian, H. H.; Meixner, A. J.; Hartschuh, A. *Phys. Rev. Lett.* **2005**, *95*, 197401.

(18) Ma, Y. Z.; Valkunas, L.; Dexheimer, S. L.; Bachilo, S. M.; Fleming, G. R. *Phys. Rev. Lett.* **2005**, *94*, 157402.

(19) Knoesel, E.; Bonn, M.; Shan, J.; Wang, F.; Heinz, T. F. *J. Chem. Phys.* **2004**, *121*, 394.

(20) Kaindl, R. A.; Carnahan, M. A.; Hagele, D.; Lovenich, R.; Chemla, D. S. *Nature* **2003**, *423*, 734.

(21) Perebeinos, V.; Tersoff, J.; Avouris, P. *Nano Lett.* **2005**, *5*, 2495.

(22) Spataru, C. D.; Ismail-Beigi, S.; Capaz, R. B.; Louie, S. G. *Phys. Rev. Lett.* **2005**, *95*, 247402.

(23) Mortimer, I. B.; Nicholas, R. J. *Phys. Rev. Lett.* **2007**, *98*, 027404.

(24) Srivastava, A.; Htoon, H.; Klimov, V. I.; Kono, J. *Phys. Rev. Lett.* **2008**, *101*, 087402.

(25) Ostojic, G. N.; Zaric, S.; Kono, J.; Moore, V. C.; Hauge, R. H.; Smalley, R. E. *Phys. Rev. Lett.* **2005**, *94*, 097401.

(26) Shaver, J.; Kono, J.; Portugall, O.; Krstic, V.; Rikken, G. L. J. A.; Miyauchi, Y.; Maruyama, S.; Perebeinos, V. *Nano Lett.* **2007**, *7*, 1851.

(27) Nish, A.; Nicholas, R. J.; Faugeras, C.; Bao, Z.; Potemski, M. *Phys. Rev. B* **2008**, *78*, 245413.

(28) Hilt, O.; Brom, H. B.; Ahlskog, M. *Phys. Rev. B* **2000**, *61*, R5129.

(29) Collins, P. G.; Bradley, K.; Ishigami, M.; Zettl, A. *Science* **2000**, *287*, 1801.

JP907195T